A single phantom to mimic ^{1}H MR Spectra of different tissues

Alejandro Bordelois Boizán [a,b,c], Giulio Gambarota [a,b], Fanny Noury [a,b], Hervé Saint-Jalmes [a,b,d]

[a] *INSERM, UMR 1099, Rennes France*

[b] *Université Rennes 1, LTSI, Rennes, France*

[c] *Universidad de Oriente, Centro de Biofísica Médica, Santiago de Cuba, Cuba*

[d] *CRLCC, Centre Eugène Marquis, Rennes, France*

Corresponding author:

Hervé SAINT-JALMES

Laboratoire Traitement du Signal et de l'Image (LTSI)

Université de Rennes 1

Campus de Beaulieu. Bât 22

35042 Cedex - Rennes - France.

Phone: +33 2 23 23 48 49

Email: herve.saint-jalmes@univ-rennes1.fr

Word Count: 3343

Number of Figures: 3

Number of references: 28

Abstract

Object To design and build a single phantom, encompassing various elementary tubes, that mimics the ^{1}H magnetic resonance (MR) spectra of liver, prostate, muscle and brain.

Materials and Methods High-resolution NMR tubes were filled with water and the metabolite of interest, at a concentration of 50 mM, or with dairy cream or oil. The tubes (5 mm outer diameter) were placed into a plastic support, the ensemble was positioned in the center of a cuboid container filled with water. Simulations of the magnetic field inhomogeneity arising from the susceptibility variations in the current phantom were also performed. MR localized spectroscopy was performed on a 1.5 T clinical scanner.

Results MR spectra of voxels positioned in four different locations of the phantom closely mimicked the resonance peaks of liver, prostate, muscle and brain *in vivo* MR spectra. In particular, for the muscle spectrum, the intramyocellular lipid (IMCL) and extramyocellular lipid (EMCL) resonances were obtained using dairy cream and oil, respectively. Simulations of the magnetic field inhomogeneity in the phantom showed that in the case of an NMR tube length five times greater than the thickness of the volume of interest, it is not necessary to fill the container with water. However, to ensure a good reception level and shim settings, the NMR tubes were immersed in water.

Conclusions A single phantom of new design, that is easily built and highly reconfigurable, is here presented, to mimic the *in vivo* MR spectra of liver, prostate, muscle, brain and other models as needed.

Keywords magnetic resonance spectroscopy, phantom, liver, prostate, brain, muscle, intramyocellular lipids,

Introduction

In the last two decades, ^{1}H magnetic resonance spectroscopy (MRS) has been successfully applied to investigations of *in vivo* metabolism in clinical and preclinical research. In order to improve metabolite quantification, it is necessary to optimize both data acquisition and data processing. As the time to perform *in vivo* experiments is limited, *in vitro* calibrations are typically needed to determine the optimal protocol/sequence parameters (such as echo time (TE), repetition time (TR), coils configuration, scan time) and to validate novel spectral editing techniques [1-3]. In order to perform these experiments, different phantoms are needed to mimic the MR spectrum of different tissues. To date, *in vivo* MRS has been mainly performed on liver, prostate, muscle and brain.

Liver contains primarily water and lipids and *in vivo* MRS experiments are mainly dedicated to quantify the lipid-to-water ratio [4]. Thus, phantoms that would model the liver MR spectrum could be made with water and oil. Since oil is not soluble in water, phantoms are made either in two separate compartments [5] or as emulsions [6,7].

In prostate, the MR spectrum of cancer tissue reveals a reduction in citrate tissue levels and often an increase in choline, compared to healthy or benign tissue [8,9]. Thus, a prostate MR phantom needs to include citrate and choline. In addition, it is preferable to add a lipid compartment, by using oil for instance, since adipose tissue surrounds the prostate and therefore contamination of spectra with lipid resonances is observed *in vivo* in certain voxels [10].

The MR spectrum of muscle tissue displays mainly choline, creatine and two groups of lipid signals that originate from the resonances of the intramyocellular (IMCL) and extramyocellular (EMCL) lipids [11,12]. The magnetic susceptibility difference between the spherical and cylindrical compartments of the IMCL and EMCL is responsible for a frequency shift of 0.2 ppm, in the case of lipid fibers parallel to the main magnetic field $\boldsymbol{B_0}$. Thus, the main lipid resonances in muscle are the IMCL peaks CH_3 and $(CH_2)_n$ at 0.9 and 1.3 ppm, respectively, and the EMCL peaks CH_3 and $(CH_2)_n$ at 1.1 and 1.5 ppm, respectively. In previous studies, emulsions (or dairy cream) and oil have been used to mimic the spectral features of IMCL and EMCL, respectively [13-15].

Brain MRS models are more complex than liver, prostate or muscle because of the larger number of metabolites involved; as a matter of fact, approximately 20 metabolites are reported in previous works performed in preclinical models [16]. The major metabolites in brain are n-acetyl-aspartate, creatine, choline, glutamate and myo-inositol.

Given the increasing interest in MRS performed with clinical and preclinical scanners, it would be advantageous to have a single phantom that can mimic the MR spectra of liver, prostate, muscle, and brain to optimize MRS protocols and pulse sequences as well as to test and validate novel acquisition techniques.

In the present study, we propose a single phantom that can be easily built and reconfigurable, and give a proof of concept that this simple system can mimic the MR spectra of liver, prostate, muscle, brain and other models as needed.

Materials and methods

Phantom

High resolution 5 mm NMR Samples Tubes™ (inner diameter of 4.20 mm, outer diameter of 4.97 mm and length of 178 mm – Ref. 502-7, NORELL Inc., NJ, USA) were filled with water and the metabolite of interest, at a concentration of 50 mM, or with dairy cream or with sunflower oil. The chemicals were purchased at Sigma-Aldrich, whereas the dairy cream and oil were bought at a local grocery shop. The tubes were placed into a plastic support with two rectangular grids of inter-element separation of 8 mm, both in horizontal and vertical direction (see Figure 1-A). The plastic support containing the NMR tubes was immersed in a cuboid plastic reservoir of dimensions $160 \times 85 \times 240$ mm^3 filled with water. A total of 49 NMR tubes can be used in the phantom, placed in a distribution of 7×7 elements.

To simulate a simplified version of the MR spectrum of different tissues, choline, citrate, creatine, lactate and n-acetyl-aspartate (NAA) were used. One metabolite (concentration of 50 mM) per tube was employed. Additional tubes were filled with dairy cream and oil, separately. It should be noted that the tubes with metabolites and oil need to be prepared once for all, but the tubes with dairy cream tubes have a shelf life of a few days.

MR Spectroscopy

For the MR spectra acquisitions, a total of 43 NMR tubes were used, placed in a rectangular distribution of 7×6 elements and one external element as a reference for imaging purposes (see Figure 1-B). All MR experiments were performed on a 1.5 T Siemens Avanto clinical system (Siemens, Germany), using a Body Matrix coil (6 elements) and a Spine Matrix coil (3 elements) for reception. Multi-slice turbo spin-echo sequences (TR=5000 ms, TE=98 ms, field of view of 190×210 mm^2, in-plane resolution of 0.6×0.6 mm^2) were acquired to position the voxel of interest (VOI) in the sample. ^{1}H MR spectra were acquired with the double spin-echo point resolved spectroscopy (PRESS) sequence [17]. The following acquisition parameters were used for all acquisitions: TR=1500 ms, TE=135 ms, 128 averages, acquisition times of 3 min 12 s, 1024 readout complex points and 1000 Hz of bandwidth. A water suppression (CHESS module [18]) was applied when acquiring prostate, brain and muscle spectra. No water suppression was applied when the phantom was used to represent the liver, as it is usually done in order to quantify the lipid-to-water ratio. The VOI dimensions ($x \times y \times z$) were different for the different acquisitions, depending on the numbers of tubes necessary to mimic the target spectrum (Figure 1-C). To mimic the liver spectrum, we used a VOI of $10 \times 20 \times 20$ mm^3 and two tubes of oil. For the acquisition of the prostate spectrum, a VOI of $30 \times 10 \times 30$ mm^3 and three tubes (citrate, choline and cream) were used. To acquire the muscle spectrum, we used a VOI of $30 \times 20 \times 20$ mm^3 and a total of six tubes (two of

choline, one of creatine, two of cream and one of oil). We acquired two spectra of brain with different VOI dimensions and tubes. One brain spectrum was acquired with six tubes (one of choline, two of creatine, two of lactate and one of NAA) and a VOI of $20 \times 30 \times 20$ mm^3 (see Figures 1-C and 2-D), and another brain spectrum with seven tubes (one additional tube of choline) and a VOI of $20 \times 40 \times 20$ mm^3.

The two brain spectra were analyzed with jMRUI [19] using the HLSVD [20] quantification method. The resonances of choline and creatine were quantified (arbitrary unit), to verify that the choline content is doubled between the two spectra while the creatine content remains stable.

Field inhomogeneity simulations

Simulations to determine the magnetic field inhomogeneity arising from the susceptibility variations in the current phantom were also performed, using the method proposed by Salomir *et al.* [21]. The dimensionless susceptibility values were taken as: $+0.36.10^{-6}$ for air, $+9.03.10^{-6}$ for water and $-11.00.10^{-6}$ for glass [22].

To assess the inhomogeneity of magnetic field, we defined h as:

$$h = \frac{\Delta B}{B_0}, \qquad \textbf{(1)}$$

where ΔB is the variation (ppm) of the magnetic field inside the VOI and B_0 is the magnetic field intensity in the center of the NMR tube. The tube inner and outer diameters used in the simulation were the same as those of the NMR tubes used in the physical phantom.

In the simulations, we considered the magnetic field inhomogeneity versus the tube-length-to-VOI-thickness ratio. The results were plotted for a tube-length-to-VOI-thickness ratio varied from 1 to 5, since for greater values the magnetic field inhomogeneity is negligible.

Results

Phantom

An illustration of the phantom is provided in Figure 1. A drawing of the plastic holder with two representative NMR tubes is shown in Figure 1-A. The cuboid plastic reservoir filled with water, in which the plastic holder and the NMR tubes were placed, is not drawn. An MR turbo spin-echo image of the phantom is shown in Figure 1-B. Here, one specific configuration with 43 NMR tubes is displayed, and the plastic reservoir filled with water is also visible. A tube was purposely positioned in a asymmetric fashion to provide a clear and immediate visual reference (Figure 1-B). The tubes filled with oil and dairy cream displayed lower signal intensity on the turbo spin-echo image, due to the T_2 relaxation time of oil and dairy cream shorter than the T_2 of water. In Figure 1-C, the VOIs that were chosen for the MRS model of liver, prostate, muscle and brain are depicted.

MR Spectroscopy

Figure 2 shows the ^{1}H MR spectra obtained in this specific configuration of the phantom. The four MR spectra closely mimicked the peak resonances of ^{1}H MR spectra of liver, prostate, muscle and brain. The MR spectrum of liver (Figure 2-A) was obtained using only the NMR tubes containing oil, as indicated also in Figure 1-C. The VOI was centered on two vertical neighbors oil tubes. We measured a line width of 1.3 Hz for this spectrum (corresponding to the half height of water peak). Due to the lower concentration of lipids in dairy cream versus oil, MR spectra acquired using a VOI centered in dairy cream did not display clearly the fat resonances in the non water-suppressed spectra. On the other hand, when the MR acquisition was performed with water suppression, it was possible to assess the lipid resonances using the dairy cream tubes and to model different lipid-to-water ratio (data not shown).

For the prostate MR spectrum (Figure 2-B), a VOI that included one tube with citrate, one tube with choline and one tube with dairy cream was used. The MR spectrum showed the characteristic lineshape of citrate at 1.5 T.

The MR spectrum of muscle (Figure 2-C) was obtained from two tubes containing dairy cream, to mimic the IMCL resonances, one tube containing oil, to mimic the EMCL resonances, two tubes with choline and one with creatine.

A simplified model of the MR spectrum of brain (Figure 2-D) was obtained with one tube of choline, one of NAA, two of lactate and two of creatine. The characteristic J-modulation of lactate, with an inverted lineshape at TE=135 ms was also observed. MR spectra acquired in VOIs close to oil tubes showed contamination from the lipid resonances into the VOI. To avoid this, it was necessary to position the oil tubes further away from the brain VOI. It should be noted that for

modeling brain MR spectra acquired close to the skull, thus with contamination from subcutaneous lipids, it would be necessary to keep one oil tube close to the chosen VOI.

For the first brain spectrum acquired using six tubes, including one tube of choline and two tubes of creatine, we obtained a quantification (arbitrary unit) of 24.0 ± 0.6 for choline and 16.7 ± 0.5 for creatine. For the second brain spectrum acquired using seven tubes, including two tubes of choline and two tubes of creatine, the resonances quantification gave the following results which are consistent with the expected values: 45.5 ± 1 and 15.6 ± 1 for choline and creatine respectively. Since these two spectra were acquired using water suppression, we can compare the resonances quantification even if the VOI dimensions were different.

Field inhomogeneity simulations

Simulations of the magnetic field inhomogeneity for the phantom proposed in the current study are shown in Figure 3. This figure shows the field inhomogeneity resulting from a distribution of magnetic susceptibility in the case of an NMR tube filled with water, and located in air or immersed in a container filled with water. We plotted the magnetic field inhomogeneity amplitude (h in ppm) versus the tube-length-to-VOI-thickness ratio (VOI dimensions in z direction), varied from 1 to 5, in case of a tube in air or immersed in water. In the case of a NMR tube length five times greater than the VOI thickness, it is not necessary to fill the container with water, since the amplitude of the magnetic field inhomogeneity are negligible. On the contrary, if the ratio between the tube length and the VOI thickness is less than 5, it is advantageous to use water to reduce this field inhomogeneity. Even if the NMR tubes used here were very long compared to the VOI thickness, filling the container with water allows to increase the signal of the phantom and to obtain enough signal to ensure a good reception level and shim settings.

Discussion

In this study we propose a single phantom that mimics the ^{1}H MR spectral features of liver, prostate, muscle and brain. The results of this study show that with the phantom proposed herein, it is possible to reproduce well the MR spectral characteristics of the tissues most commonly investigated with *in vivo* MRS.

There are a number of useful features in this phantom: first, it is possible to change quickly its configuration, as the NMR tubes can be easily added to or removed from the phantom. This could be particularly useful in calibration experiments, when it is necessary to test many different scenarios. The quick modification of the phantom configuration is a clear advantage of it over manufactured or homemade phantoms previously proposed. As a matter of fact, phantoms provided by the MR scanner vendors cannot be modified and typically contain only a very limited number of metabolites. It should be noted that the number of metabolites that are quantifiable with confidence (using the generally accepted criterion of a Cramér–Rao lower bound < 20% [23], for instance) has substantially increased in the last two decades, and detection of 'novel' metabolites is an active field of MR research. In this context, this phantom could be useful for testing data acquisition or processing techniques for spectral editing.

The metabolite concentration as a function of the VOI dimensions can be determined by the following argument: due to the translation symmetry of this phantom along the *z* direction (which is also the direction of the static magnetic field and corresponds to the NMR tube orientation in the scanner), a 3D volume problem is reduced to 2D surface problem. Thus, the metabolite concentration in a VOI can be written as a surface ratio:

$$c_{VOI} = c_{tube}\frac{\pi D^2}{4VOI_x VOI_y}, \qquad (2)$$

where c_{VOI} and c_{tube} are the metabolite concentration in the VOI and in the NMR tube, respectively, D is the NMR tube diameter, VOI_x and VOI_y are the VOI dimensions in x and y directions, respectively. In this equation the NMR tube thickness is assumed negligible.

The NMR tubes were filled with metabolite concentrations (50 mM) higher than the typical biological concentrations (1 to 10 mM). This is necessary since the water surrounding the NMR tubes virtually dilutes the metabolite concentration in a given VOI. As shown in the Equation 2, the metabolite concentration in a VOI can be simply controlled by changing the VOI dimensions (x and/or y direction(s)). For instance, when reducing the VOI size, that is, decreasing in the VOI the volume of water surrounding the NMR tube, the effective metabolite concentration increases.

Though not used in the current work, Equation 2 is here provided for calculations of metabolite concentrations in future studies. It should be stressed, however, that great care must be always taken in the determination of absolute metabolite concentrations, when accounting for multiple confounding factors such as relaxation times and signal modulations due to J-coupling play.

In the liver model, the lipid-to-water ratio was changed by increasing or reducing the VOI size around the NMR tubes containing oil (or dairy cream), so to keep the oil volume constant and change the water volume in the VOI (date not shown). With this approach, the quantification error on the fat content is introduced primarily by the VOI selection profile of the pulse sequence. An alternative to this approach is to prepare different phantoms (for instance, different emulsions) with different fat content, as proposed in previous works [24,25]; in this case however, the quantification errors in MRS come from the phantom preparation (amount of fat in each emulsion, homogeneous distribution of fat in the phantom, etc.).

In general, it should be also noted that, due to the translation symmetry of this phantom, it is possible to increase the signal-to-noise ratio without varying the concentration ratios by increasing the VOI dimension (*z* direction), to a limit that will not degrade the spectral resolution.

In recent years, there has been a growing interest in lipids quantification with MRS, with particular attention to the quantification of IMCL. A number of dedicated phantoms have been previously proposed for mimicking the *in vivo* muscle MR spectrum. The main differences among phantoms proposed in different studies [26] are the geometry/design and the substances used to mimic the lipid resonances. For instance, Szczepaniak *et al.* [15] used a concentric vials configuration, one vial filled by soybean oil inside another vial filled by Intralipid^{TM}. Cui *et al.* [13] use two screw cap vials filled by soybean oil, inside a box filled by Intralipid^{TM}. Ren *et al.* [26] designed an agar gel phantom with oil-soaked paper rolls mimicking EMCL and oil droplets swirled into the gel to mimic IMCL. In another study [14], dairy cream was used to model the IMCL resonances, and dairy cream and oil were poured in the same cylindrical container. In the current study, dairy cream [27,28] was preferred to the much more expensive Intralipid^{TM} to mimic IMCL and sunflower oil was used to mimic EMCL; dairy cream and oil were each put in separate NMR tubes. The muscle model reproduced well the MR spectral characteristics of *in vivo* muscle MRS, i.e., the resonance peaks of IMCL and EMCL. It should be noted that here the muscle MR spectrum model is achieved in the same phantom with liver, prostate and brain models.

A simulation of the magnetic field properties of the current phantom was also conducted. Typically, a spherical shape design is used in MR phantoms, because this geometry generates less magnetic field inhomogeneity than cuboid or cylindrical shapes. The external shape of the phantom proposed in the current study is not spherical, as the NMR tubes are placed in the center a cuboid container filled with water. The choice of a cuboid container was due to the fact containers with this shape are

commonly found. The container was large enough so that the magnetic field inhomogeneity at the water-air interface did not affect the line width of the spectra acquired from each VOI. For the experiments of the current study, the cuboid container (in which the NMR tubes were positioned) was filled with water. This was necessary in order to obtain enough signal for the scanner automatic adjustments (transmitter frequency, receiver gain, shimming). Furthermore, the presence of water in the container allows to dilute and thus control the metabolite concentration in a VOI. Simulations of the magnetic field inhomogeneity, however, showed that from a strictly magnetostatic point of view, for a VOI thickness five times smaller than the NMR tube length, there was no difference between having the NMR tubes in air or immersed in water.

Another useful feature of this phantom is that the simple yet accurate geometrical arrangement of the NMR tubes allows for verification that the actual location of the VOI corresponds to the one prescribed by the user. This feature could be useful to validate the localization accuracy of chemical shift imaging (CSI) sequences, by adjusting the voxel size so to include only one tube per voxel, and to assess the signal contamination from nearby voxels. Furthermore, it should be noted that a similar phantom could be also designed for preclinical MR scanners, using thinner NMR tubes (diameter of 3 mm).

Conclusion

In this study, a single phantom of new design, that is easily built and highly reconfigurable, is presented, to mimic the *in vivo* MR spectra of liver, prostate, muscle, brain and other models as needed.

Acknowledgements

The authors thank the French Embassy in Cuba for its support to this project.

References

1. Thompson RB, Allen PS. *Response of metabolites with coupled spins to the STEAM sequence.* Magn Reson Med (2001). **45**: 955-965.
2. Snyder J, Wilman A. *Field strength dependence of PRESS timings for simultaneous detection of glutamate and glutamine from 1.5 to 7 T.* J Magn Reson (2010). **203**:66-72.
3. Mescher M, Merkle H, Kirsch J, Garwood M, Gruetter R. *Simultaneous in vivo spectral editing and water suppression.* NMR Biomed (1998). **11**:266-272.
4. Szczepaniak LS, Babcock EE, Schick F, Dobbins RL, Garg A, Burns DK, McGarry JD, Stein DT. *Measurement of intracellular triglyceride stores by 1H spectroscopy: validation in vivo*. Am J Physiol (1999). **276**:E977-989.
5. Hussain HK, Chenevert TL, Londy FJ, Gulani V, Swanson SD, McKenna BJ, Appelman HD, Adusumilli S, Greenson JK, Conjeevaram HS. *Hepatic fat fraction: MR imaging for quantitative measurement and display-early experience*. Radiology (2005). **237**:1048-1055
6. Hamilton G, Yokoo T, Bydder M, Cruite I, Schroeder ME, Sirlin, CB, Middleton MS. *In vivo characterization of the liver fat 1H MR spectrum*. NMR Biomed (2011). **24**:784-790.
7. Leporq B, Ratiney H, Pilleul F, Beuf O. *Liver fat volume fraction quantification with fat and water T1 and T2* estimation and accounting for NMR multiple components in patients with chronic liver disease at 1.5 and 3.0 T*. Eur Radiol (2013). **23**:2175-2186.
8. Kurhanewicz J, Vigneron DB, Nelson SJ, Hricak H, MacDonald JM, Konety B, Narayan P. *Citrate as an in vivo marker to discriminate prostate cancer from benign prostatic hyperplasia and normal prostate peripheral zone: detection via localized proton spectroscopy.* Urology (1995). **45**:459-466.
9. van der Graaf M, van den Boogert HJ, Jager GJ, Barentsz JO, Heerschap A. *Human prostate: multisection proton MR spectroscopic imaging with a single spin-echo sequence-preliminary experience.* Radiology (1999). **213**:919-925.
10. Scheenen TW, Klomp DW, Röll SA, Fütterer JJ, Barentsz JO, Heerschap A. *Fast acquisition-weighted three-dimensional proton MR spectroscopic imaging of the human prostate.* Magn Reson Med (2004). **52**:80-88.
11. Boesch C, Slotboom J, Hoppeler H, Kreis R. *In vivo determination of intra-myocellular lipids in human muscle by means of localized 1H-MR-spectroscopy*. Magn Reson Med (1997). **37**:484-493.
12. Schick F, Eismann B, Jung WI, Bongers H, Bunse M, Lutz O. *Comparison of localized proton NMR signals of skeletal muscle and fat tissue in vivo: two lipid compartments in muscle tissue.* Magn Reson Med (1993). **29**:158-167.
13. Cui MH, Hwang JH, Tomuta V, Dong Z, Stein DT. *Cross contamination of intramyocellular lipid signals through loss of bulk magnetic susceptibility effect differences in human muscle using ^{1}H-MRSI at 4 T*. J Appl Physiol (2007). **103**:1290-1298.
14. Gambarota G, Janiczek RL, Mulkern RV, Newbould RD. *An NMR Phantom Mimicking*

Intramyocellular (IMCL) and Extramyocellular Lipids (EMCL). Appl Magn Reson (2012). **43**:451-457.

15. Szczepaniak LS, Dobbins RL, Stein DT, McGarry JD. *Bulk magnetic susceptibility effects on the assessment of intra- and extramyocellular lipids in vivo*. Magn Reson Med (2002). **47**:607-610.
16. Pfeuffer J, Tkác I, Provencher SW, Gruetter R. *Toward an in vivo neurochemical profile: quantification of 18 metabolites in short-echo-time 1H NMR spectra of the rat brain.* J Magn Reson (1999). **141**:104-120.
17. Bottomley PA. *Selective volume method for performing localized NMR spectroscopy.* US Patent (1984). 4, 480, 228.
18. Haase A, Frahm J, Hänicke W, Matthaei D. *1H NMR chemical shift selective (CHESS) imaging*. Phys Med Biol. (1985). **30**:341-4.
19. Naressi A, Couturier C, Devos JM, Janssen M, Mangeat C, de Beer R, Graveron-Demilly D. *Java-based graphical user interface for the MRUI quantitation package.* MAGMA (2001). **12**:141-52.
20. Pijnappel WWF., van den Boogaart A, de Beer R, van Ormondt D. *SVD-based quantification of magnetic resonance signals.* J Magn Res (1992). **97**: 122-134.
21. Salomir R, de Senneville BD, Moonen CT. *A fast calculation method for magnetic field inhomogeneity due to an arbitrary distribution of bulk susceptibility.* Concepts Magn Reson (2003). **19B**:26-34.
22. Schenck JF. *The role of magnetic susceptibility in magnetic resonance imaging: MRI magnetic compatibility of the first and second kinds*. Med Phys (1996). **23**: 815-850.
23. Provencher SW. *Estimation of metabolite concentrations from localized in vivo proton NMR spectra*. Magn Reson Med (1993). **30**:672-679.
24. Ballweg V, Wojtczyk H, Roth N, Martirosian P, Springer F, Schick F. *Optimized in-phase and opposed-phase MR imaging for accurate detection of small fat or water fractions: theoretical considerations and experimental application in emulsions*. Magn Reson Mater Phy (2011). **24**:167-178.
25. Hu HH, Nayak KS. *Change in the proton T1 of fat and water in mixture*. Magn Reson Med (2010). **63**:494-501.
26. Ren J, Sherry AD, Malloy CR. 1H MRS of intramyocellular lipids in soleus muscle at 7 T: spectral simplification by using long echo times without water suppression. Magn Reson Med (2010). **64**:662-671.
27. Jones C, MacKay A, Rutt B. Bi-exponential T2 decay in dairy cream phantoms. Magn Reson Imaging (1998). **16**:83-85.
28. Mulkern RV, Hung YP, Ababneh Z, Maier SE, Packard AB, Uluer MC, Kacher DF, Gambarota G, Voss S. *On the strong field dependence and nonlinear response to gadolinium contrast agent of proton transverse relaxation rates in dairy cream*. Magn Reson Imaging (2005). **23**:757-764.

Figure & Legends

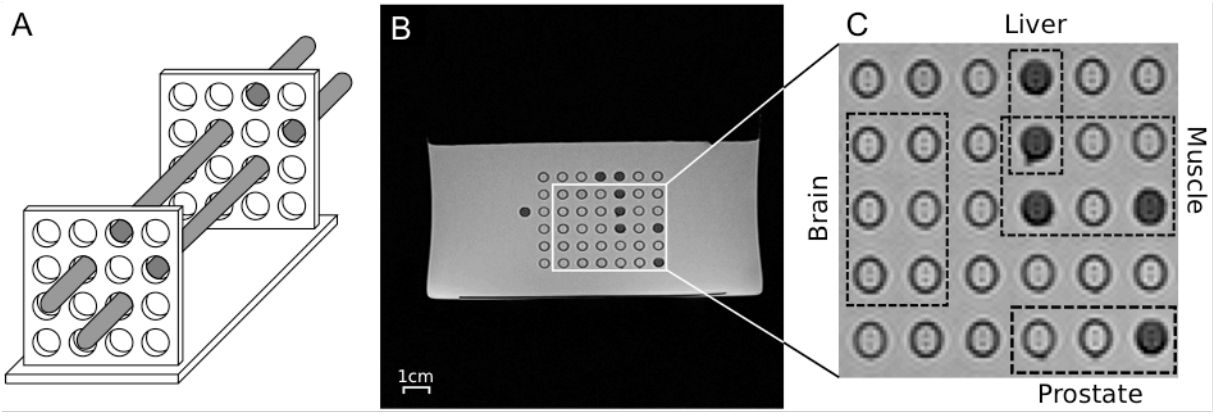

Figure 1.

Presentation of the phantom design. A drawing of the plastic holder with two representative NMR tubes (A), an MR turbo spin-echo image of the whole phantom (B), and the location of the VOIs (C) chosen for the MRS model of liver, prostate, muscle and brain are depicted.

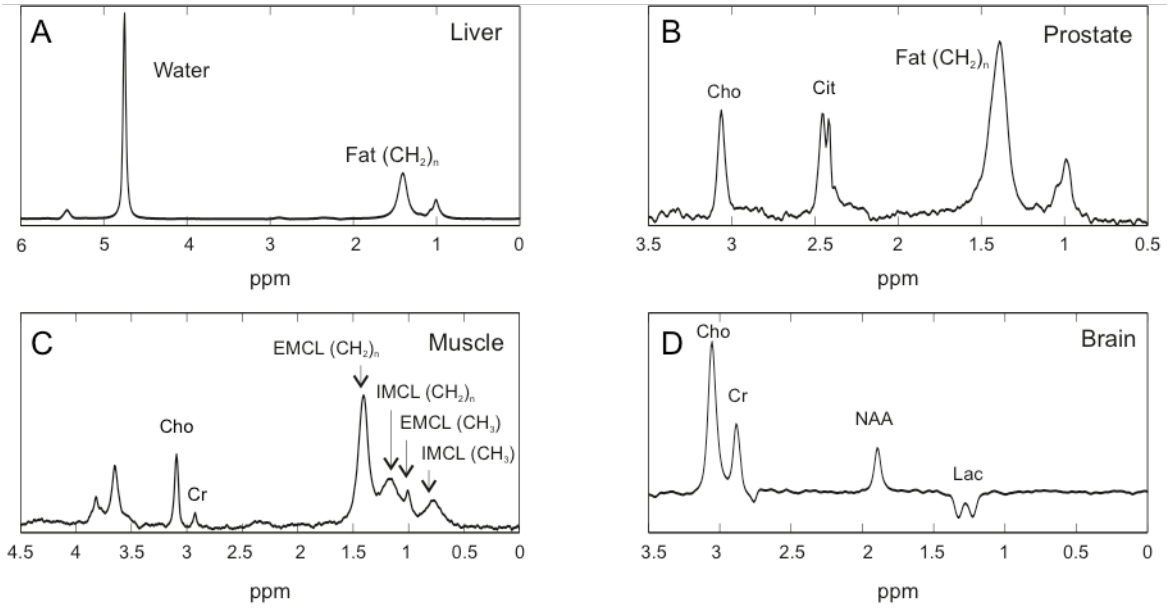

Figure 2.

^{1}H MR PRESS spectra of four VOIs (the position of each VOI is depicted in the Figure 1). The four MR spectra mimic well the spectral features of liver (A), prostate (B), muscle (C) and brain (D) *in vivo* MR spectra. The resonances of choline (Cho), citrate (Cit), creatine (Cr), lactate (Lac), n-acetyl-aspartate (NAA), intramyocellular lipid (IMCL), extramyocellular lipid (EMCL), water and fat were labeled.

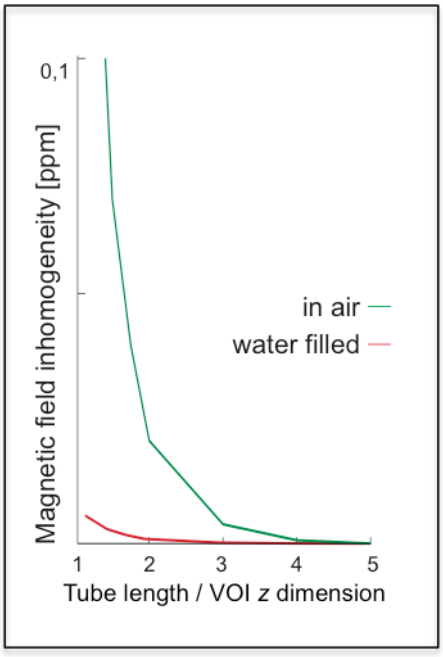

Figure 3.

Simulations of the magnetic field inhomogeneity in the phantom. We plotted the magnetic field inhomogeneity amplitude (*h* in ppm) versus the tube-length-to-VOI-thickness ratio (VOI dimensions in *z* direction), varied from 1 to 5. Two situations were considered: the NMR tube in air or immersed in water. In the case of a NMR tube length five times greater than the VOI thickness, it is not necessary to fill the container with water, since the amplitude of the magnetic field inhomogeneity are negligible. On the contrary, if the ratio between the tube length and the VOI thickness is less than 5, it is advantageous to use water to reduce this field inhomogeneity. However, it is necessary to fill the container with water to increase the signal of the phantom and to obtain enough signal to ensure a good reception level and shim settings.